Available online at www.sciencedirect.com
SCIENCE DIRECT
Sensors and Actuators A 123–124 (2005) 210–215
SENSORS AND ACTUATORS A PHYSICAL
www.elsevier.com/locate/sna

A double heater integrated gas flow sensor with thermal feedback

Paolo Bruschi [a,*], Alessandro Diligenti [a], Dino Navarrini [b], Massimo Piotto [c]

[a] *Dipartimento di Ingegneria dell'Informazione, via G. Caruso, I-56122 Pisa, Italy*
[b] *STMicroelectronics, R&D Division, via Olivetti 2, I-20041 Agrate Brianza (MI), Italy*
[c] *IEIIT-Sezione di Pisa, CNR, via G. Caruso, I-56122 Pisa, Italy*

Received 13 September 2004; received in revised form 12 April 2005; accepted 19 April 2005
Available online 9 June 2005

Abstract

An integrated thermal sensor for flow rates below 200 sccm, consisting of two central heaters and two thermopiles, located downstream and upstream with respect to the heaters, is presented. The sensor, fabricated by post-processing chips produced with a standard microelectronic process, is operated in closed loop configuration through a single operational amplifier, in such a way that the flow-induced temperature difference between the two thermopiles is cancelled by applying a power mismatch to the two heaters. The output signal is proportional to the heater power unbalance. Static and dynamic electrical characterization of the sensor is performed. The response to nitrogen flow rates has been measured for various gas pressures.

Keywords: Integrated sensors; Flow sensors; Pressure effects; Micromachining

1. Introduction

Thermal sensors can be used both for the direct measurement of thermal quantity, such as heat and temperature and as indirect transducers to convert quantity, such as pressure, acceleration, radiation into an electrical signal through a thermal effect. Their integration on a silicon chip has become feasible with the development of micromachining techniques which allowed the fabrication of micrometric structures thermally insulated from the substrate [1]. In this way, thermal sensors with improved sensitivity and time response have been developed. Integrated thermal sensors have been largely used to perform fluid flow measurements and are usually preferred to mechanical transducers, due to their intrinsic structural simplicity and reliability [2]. They can be divided into three main categories [3]: (i) anemometers, (ii) differential calorimetric flow sensors and (iii) time of flight sensors. Anemometers are based on the measurements of the flow-induced variation of the convective thermal conductance between a hot element and the fluid. They usually suffer from non-linearity in the response and sensitivity threshold due to the transition from free to forced convection [4]. Differential calorimetric flow sensors detect the heat amount transported by the fluid and they are usually made up of a heater positioned between an upstream and a downstream temperature probe while the output signal is the temperature difference [5]. Time of flight sensors measure the time taken by a heat pulse to cover a known distance and their sensitivity is very low at small flow rates [3]. The low sensitivity to parasitic thermal paths and the virtual absence of offset, due to the symmetrical structure of differential calorimeters, facilitate their use as precision flow meters.

In this work, we propose a flow sensor that uses the thermal conductance between heaters and temperature probes as feedback path of the readout amplifier, thus eliminating the need of passive components. The sensor structure, as schematically shown in Fig. 1, is similar to the differential calorimetric configuration with the exception of splitting the heater into two thermally insulated sections. The two heaters are polysilicon resistors positioned on individual silicon dioxide membranes, suspended by means of 45° inclined arms. The temperature probes are two thermopiles, one upstream and the other downstream with respect to the heaters, with

* Corresponding author. Tel.: +39 050 2217538; fax: +39 050 2217522.
E-mail address: p.bruschi@iet.unipi.it (P. Bruschi).

0924-4247/$ – see front matter © 2005 Elsevier B.V. All rights reserved.
doi:10.1016/j.sna.2005.04.023

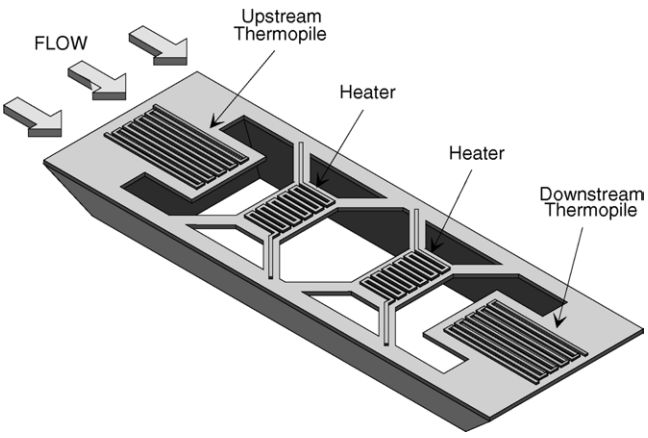

Fig. 1. Schematic view of the device.

the hot contacts located at the extreme of a silicon dioxide cantilever beam and the cold contacts on bulk silicon. In practice, the two heaters are driven differentially by a feedback loop that forces the two probe temperatures to be equal also in the presence of the flow and the resulting unbalance of the heater drive is the output signal of the sensor. This configuration is similar to that presented in Ref. [6], where it is proposed as a possible method to overcome the nonlinearity of temperature sensor. An interesting application of this principle is the two axis wind sensor described in Ref. [7], designed to measure air speeds in the range of several meters per second using a completely standard CMOS chip.

The novelty of our solution stands in the simplicity of the electronic interface, reduced in practice to a single operational amplifier connected in such a way that the resulting sensitivity is fixed by thermal conductances, with no need of precise passive components. This property simplifies the development of compact integrated cells consisting of a flow sensor and its interface electronics.

2. Device fabrication

The device was designed with the BCD3S process of STMicroelectronics, a process including bipolar, CMOS (1 μm) and DMOS active devices, with two polysilicon levels and three metal layers. Fig. 2(a) shows the layout of the 180 μm × 580 μm structure. The two heaters are 4.8 kΩ polysilicon resistors while the thermopiles are formed by 20 n^+-poly/Al thermocouples. The cantilever beams are 35 μm long and 85 μm wide while the rectangular membranes are 45 μm long and 60 μm wide; the cantilever beam versus membrane distance is 60 μm while the distance between the two membranes is 110 μm. Thermal insulation of the structures from the substrate is provided by a cavity in the silicon obtained by means of a post-processing technique [1] consisting in silicon etching applied to the front side of standard chips, fabricated by the silicon foundry.

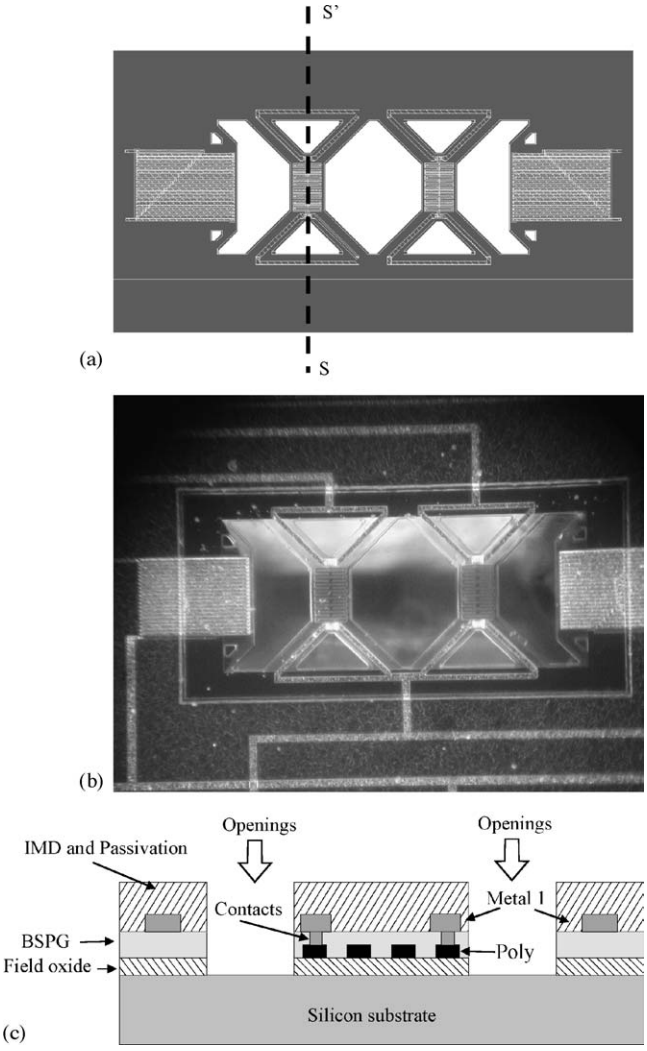

Fig. 2. (a) Layout of the device, (b) microphotograph of the device after selective silicon removal and (c) cross-sectional view along S–S′ after removal of the metal 2 and metal 3 patches from the openings.

To this purpose, openings, shown as white areas in Fig. 2(a), in all the oxide layers had to be included in the layout, stacking passivation opening, vias, contact and active area layers. To avoid photoresist accumulation due to the resulting deep holes, metal 2 and metal 3 patches have been placed over the openings. In this way, the lithographic problems occurring during chip fabrication are reduced and the metal patches can be easily removed in the post-processing phase.

A 4 μm resolution photolithography step was used to protect the pads during the aluminium etching. Alignment of the mask to the chip was not critical due to the large distance between the pads and the active structures. Note that, according to the layout, the passivation layer was removed by the foundry only over the pads and the cavities intended for allowing the successive silicon etching. As a result, all the metal 2 and metal 3 interconnects were not affected by the first post-processing etching.

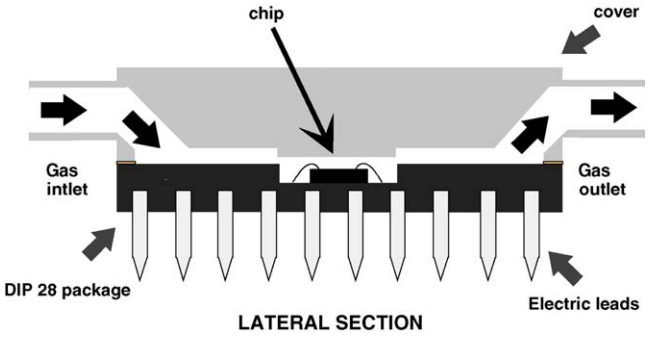

Fig. 3. Package used to connect the sensor to a gas line.

After the aluminium etch, performed with a standard H_3PO_4, HNO_3 and CH_3COOH water mixture, the silicon substrate was directly accessible through cavities properly designed to obtain the final structure. A cross-sectional view of the openings after removal of the metal patches is shown in Fig. 2(c). Silicon removal was accomplished by means of an EDP solution type "S" [8] at 115 °C for 105 min with a silicon etch rate of about 45 μm/h. Among the available wet silicon etchings for post-processing, KOH is usually used for backside etching with the front side being protected by mechanical housing and/or polymer coatings [9]. TMAH solutions, with a proper amount of silicon and ammonium peroxodisulfate dissolved, have been also proposed as CMOS compatible silicon etching [10] though for long time etchings the solution must be refreshed frequently and is very critical [11]. On the other hand, EDP solutions are readily masked by SiO_2 and Si_3N_4 and their etching characteristics remain stable for a long time if contact with oxygen atmosphere is avoided [8]. Furthermore, the solution type "S" has the property of etching aluminium at a very slow rate, about 180 times slower than silicon, allowing to etch CMOS chips up to 4 h without any pad protection [12]. Problems deriving from the toxicity of EDP solutions have been circumvented performing the etch into a sealed environment.

In Fig. 2(b), an optical microscope photograph of the device after the silicon removal in shown: the cavity in the substrate under the suspended SiO_2 membranes and cantilever beams are clearly visible.

The sensor has been packaged and bonded into a standard DIP28 case. A polymetylmethacrylate cover has been glued to the top of the case by means of epoxy resin, in order to expose the chip surface to the gas flow. The package is schematically shown in Fig. 3. The cover includes two channels used as inlet and outlet for the gas stream. The channels convey the gas into the small chamber that hosts the chip; 1 cm long upstream and downstream horizontal sections have been included to make the gas flow parallel to the chip surface. Stainless steel pipes of 1/4′ diameter were fit and sealed to the cover to provide easy connection to the gas line.

3. Device operating principle

Fig. 4 shows the typical configuration used to drive the flow sensors. The power dissipation of the two heaters, R_{T_1} and R_{T_2} in the figure, will be indicated with P_1 and P_2, respectively. The op-amp is powered by a single power supply indicated with V_{DD}. Resistors R_A and R_B produce the input common mode voltage (V_{CM}) required by the op-amp. The V_{CM} value, fixed to $V_{DD}/2$ in this work, is clearly not critical; therefore, no particular precision or matching characteristics are required for R_A and R_B.

The signals V_{T_1} and V_{T_2} indicate the thermopile outputs. The thermal connection between the heaters and the thermopiles constitutes the feedback of the circuit. Considering that $R_{T_1} = R_{T_2} = R_T$, the relationship between P_1, P_2 and V_{out} is given by:

$$P_2 = \frac{V_{out}^2}{R_T}, \qquad P_1 = \frac{(V_{DD} - V_{out})^2}{R_T},$$
$$P_1 - P_2 = 2\frac{V_{DD}}{R_T}\left(\frac{V_{DD}}{2} - V_{out}\right) \tag{1}$$

If the flow is zero, and $P_1 = P_2$, symmetry arguments suggest that the two thermopiles are at the same temperature, so that the op-amp input is null. Considering for simplicity that the op-amp offset is zero, then $V_{out} = V_{DD}/2$. This, in turn, leads again to $P_1 = P_2$ proving that this is a valid state of the system.

When a flow is applied, the downstream thermopile tends to reach a temperature higher than the upstream one. So a differential input is applied to the amplifier producing a power unbalance to the heaters. If the polarity of thermopile connection is such that the feedback is negative, this power unbalance tends to re-equilibrate the temperatures. The difference ΔV_{out} between the actual output voltage and the value it assumes in rest conditions (ideally $V_{DD}/2$ resulting in $P_1 = P_2$) represents the output signal.

Assuming that heat transfer occurs mainly through conduction and forced convection, a linear relationship exists between the temperatures T_1 and T_2, at the edge of the two cantilevers, and the heater powers P_1 and P_2. Therefore, the

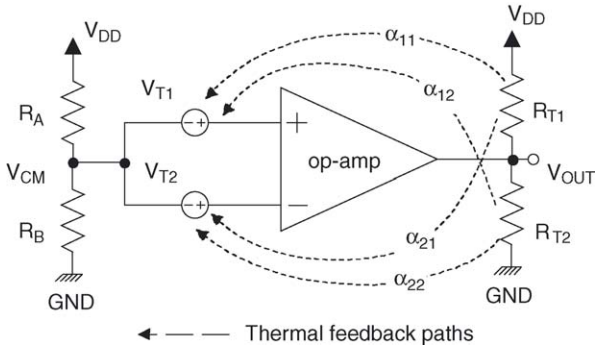

Fig. 4. Schematic view of the circuit used to drive the sensor.

following equations hold:

$$\begin{cases} V_{T_1} = \alpha_{11} P_1 + \alpha_{12} P_2 \\ V_{T_2} = \alpha_{21} P_1 + \alpha_{22} P_2 \end{cases} \quad (2)$$

where α_{ij} are flow dependent coefficients that include also the thermopile sensitivity, corresponding to the thermal feedback paths shown in Fig. 4. Since, due to the way the thermopile has been designed, all the coefficients are positive and, reasonably, $\alpha_{11} > \alpha_{12}$ and $\alpha_{22} > \alpha_{21}$, it can be easily shown that negative feedback is present. If the loop gain is large enough, it can be easily shown that the difference $V_{T_1} - V_{T_2}$ is practically equal to the amplifier input offset voltage V_{io}. From equation (2), we have:

$$V_{\text{io}} + P_2(\alpha_{22} - \alpha_{12}) = P_1(\alpha_{11} - \alpha_{21}) \quad (3)$$

By symmetry arguments, it can be argued that the terms in parenthesis can be written as a function of flow, Q, such that:

$$(\alpha_{22} - \alpha_{12}) = f(Q); \qquad (\alpha_{11} - \alpha_{21}) = f(-Q) \quad (4)$$

Substituting the first-order Taylor approximation for the function $f(Q)$ into equation (3), we get:

$$(P_1 - P_2) f(0) = (P_1 + P_2)\beta Q + V_{\text{io}} \quad (5)$$

where β is $\mathrm{d}f/\mathrm{d}Q$ calculated for $Q = 0$. According to equation (1), $P_1 - P_2$ is linearly proportional to the voltage difference $\Delta V_{\text{out}} = V_{\text{out}} - V_{\text{DD}}/2$. Now, considering that, for small deviations of V_{out} from $V_{\text{DD}}/2$, $P_1 + P_2$ is nearly constant and equal to $V_{\text{DD}}^2/2R_T$, we obtain:

$$\Delta V_{\text{out}} = -\frac{\beta V_{\text{DD}}}{4 f(0)} Q + \frac{R_T}{2 V_{\text{DD}} f(0)} V_{\text{io}} \quad (6)$$

Note that, if the offset is zero, the heater resistance R_T has no effect on the sensor law, provided that the downstream and upstream resistors are identical. In addition to process errors, a possible source of mismatch can be the temperature difference between the two heaters in the presence of flow. Due to the low temperature coefficient of the polysilicon used in our devices (<500 ppm/K), this effect was neglected. As far as the amplifier offset is concerned, the corresponding error in terms of measured flow, Q_{io}, can be easily derived from equation (6):

$$Q_{\text{io}} = V_{\text{io}} \frac{2R_T}{V_{\text{DD}}^2 \beta} \quad (7)$$

The sensor can be operated as a conventional calorimeter in an open loop configuration, in which both heaters are driven with the same constant power P and the thermopile output $V_{T_1} - V_{T_2}$ is the output signal. Using equation (2), we get:

$$V_{T_1} - V_{T_2} = P(\alpha_{11} - \alpha_{21}) - P(\alpha_{22} - \alpha_{12}) = -2P\beta Q \quad (8)$$

In this case, the offset of the amplifier used to read the signal produces an error equal to $Q_{\text{io}} = V_{\text{io}}/(2P\beta)$. If P is the same as in the closed loop configuration (in the particular condition $P_1 = P_2$), we obtain again equation (7), i.e. in open or closed loop configuration the amplifier offset has the same effect on the measurement precision. A similar analysis can be performed for the pass-band noise. This led us to use a low noise, low offset op-amp, the Analog Devices OP07, powered with a 12 V supply voltage. It should be noted that a conventional differential calorimetric flow sensor requires a high gain instrumentation amplifier where precision resistors are used to set the gain. Our solution simplifies the interface design since the gain is intrinsically set by the thermal feedback represented by the parameters α_{ij}.

4. Experimental results

Preliminary electrical measurements have been devoted to characterize the static and dynamic response of the thermopile output to variations of the voltage V_{out}. These tests were required to estimate the frequency response of the sensor in order to verify the stability of the closed loop configuration of Fig. 4.

During these experiments, the thermopile output was read by a purposely built low noise–low offset amplifier based on an Analog Devices AD620 instrumentation amplifier with a gain of 100. The heaters were still connected as in Fig. 4 but the heater common terminal (V_{out}) was driven by a waveform generator instead of the op-amp. The result is shown in Fig. 5 which refers to an experiment performed in still air at room temperature.

The excellent linearity can be explained considering that, in condition of zero flow, the temperature difference $T_1 - T_2$ is proportional to the difference $P_1 - P_2$ and that the latter is linearly proportional to $V_{\text{out}} - V_{\text{DD}}/2$, as shown in the previous section.

In Fig. 6, we have shown the response of the device to a 80 Hz square wave applied to the terminal V_{out}. The estimated time constant is nearly 0.7 ms, corresponding to a upper band limit of 220 Hz. The dominant pole of the feedback loop, obtained mounting the sensors in its operating configuration

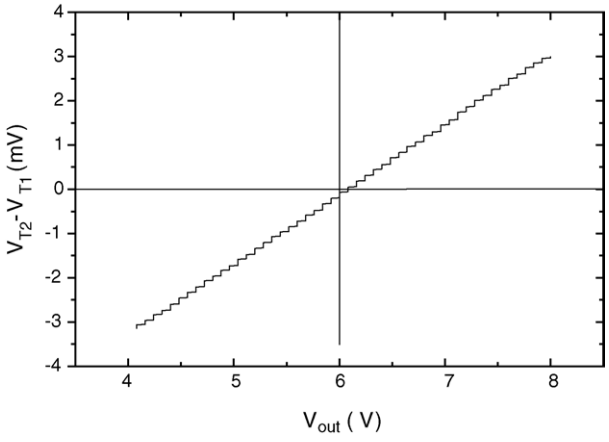

Fig. 5. Static response of the thermopile output as a function of heater unbalance.

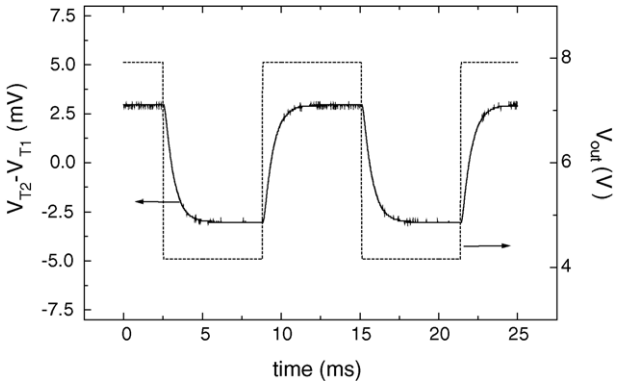

Fig. 6. Thermopile output induced by applying a square wave to the common terminal of the heaters.

(Fig. 4), is then given by the op-amp open loop dominant pole (around 3 Hz). Using a two pole approximation of the loop gain, a phase margin of 25° has been estimated, just sufficient to guarantee stability with no need of additional components.

The sensor response to a nitrogen flow was measured by connecting the packaged sensor to a standard gas line, equipped with precise mass flow controller (MKS 1179 B) and flow meter (MKS 179 B). The sensor inlet and outlet could also be connected to a pressure gauge (MKS Baratron 750 B) by means of ball valves, in order to monitor the downstream and upstream pressure.

The measurements were performed at room temperature using the electrical configuration of Fig. 4.

The experiments were repeated for various pressure values from atmospheric pressure to 120 mbar. The pressure was varied by connecting the gas line outlet to a rotary pump through a pin valve and tuning the latter in order to stabilize the pressure to the desired value. This operation was repeated for each flow rate setting. No difference between the upstream and downstream pressure was detected, indicating that the sensor insertion loss was negligible within the instrument resolution (1 mbar) over the explored flow rate range. Typical results are shown in Fig. 7, where the difference between the actual and rest value of the output voltage is plotted against the flow rate.

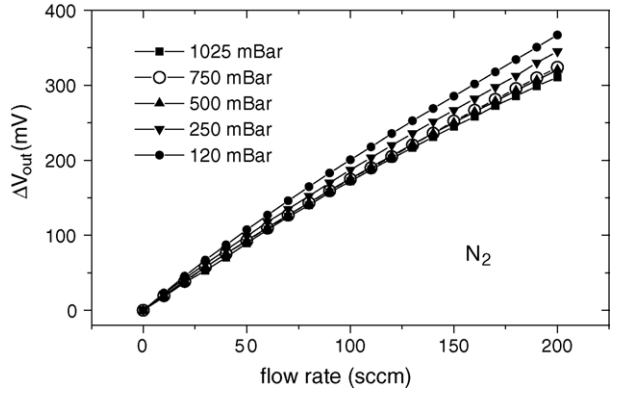

Fig. 7. Response of the sensor to nitrogen flow rates at various pressures. The sensor was mounted in its closed loop operating configuration.

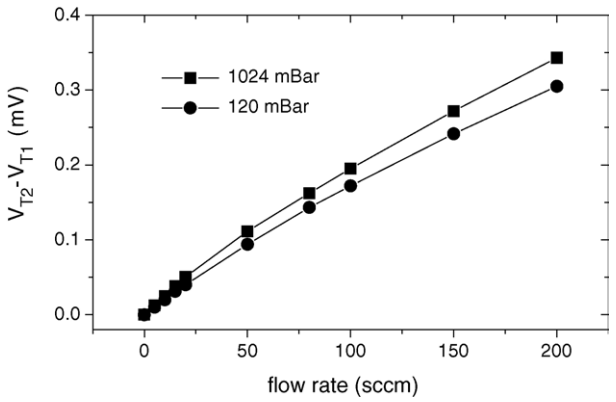

Fig. 8. Thermopile output difference as a function of nitrogen gas flow at two pressure values when both heaters are supplied with the same constant voltage (6 V).

Note that, as resulting from Fig. 5, the unavoidable asymmetries in the sensor structure, due to matching errors in the fabrication process, make the rest voltage to differ from the theoretical value $V_{DD}/2$. Deviations from the linear fit are less then 4% of full scale for the curve at 1025 mbar, indicating that the first-order approximation introduced to derive equation (4) is acceptable in the whole flow rate interval. As far as the effects of pressure are concerned, it can be observed that the response to flow does not significantly change when the pressure is reduced from 1025 to 500 mbar. A progressive sensitivity increase can be observed for pressures lower than 500 mbar. To understand this behavior, it is useful to consider equation (6) which indicates a linear proportionality between the sensitivity and the ratio $\beta/f(0)$. Calculations of the pressure dependence of the parameter β is not straightforward, since it involves heat transfer between two solid surfaces due a fluid in forced convection conditions, with characteristic lengths comparable to the molecules free path. For this reason, we have experimentally determined the effect of pressure on the parameter β, by feeding the two heaters with the same constant power P and reading the thermopile voltage difference as a function of flow. In these conditions, corresponding to operate the sensor as a standard differential calorimeter, the output $V_{T_1} - V_{T_2}$ is given by equation (8).

The results are shown in Fig. 8 for two pressure values, where it is apparent that β is smaller at lower pressures. On the other hand, the factor $f(0)$ is proportional to the thermal conductance between two solid surfaces due to a gas in rest conditions, i.e. it is due to conduction and, possibly, to free convection mechanisms. An indication of its pressure dependence can be found in Ref. [13] for a similar structure used as a pressure gauge. A reduction of the factor $f(0)$ when the pressure is decreased is reported. The overall sensitivity increase observed in our sensor in closed loop configuration indicates that, when the pressure diminishes, $f(0)$ decrease at a faster rate than β. The reduction of the sensitivity to pressure variations exhibited at higher pressures can be reasonably ascribed to the molecule mean free path becoming smaller than the structure dimensions.

5. Conclusions

The proposed thermal flow sensor proved very effective in reducing the required electronic readout circuit to a minimum. A full scale output range of 400 mV has been achieved using a single operational amplifier with no need of precise passive feedback components. The response was monotonic with reduced deviations from linearity over the whole explored flow rate range. Cross-sensitivity to pressure was satisfactorily low over 500 mbar. For lower pressures, a sensitivity increase was observed, in contrast with the sensitivity decrease occurring when the sensor is operated as a conventional differential calorimetric flow sensor. This can be considered as a consequence of adopting a configuration were also the feedback path is pressure dependent.

Acknowledgements

This work was partially supported by the Italian Space Agency (ASI) and by the *Fondazione Cassa di Risparmio di Pisa*. The authors also wish to thanks the STMicro electronics R&D group of Cornaredo (MI) for fabricating the test chip.

References

[1] H. Baltes, O. Paul, O. Brand, Micromachined thermally based CMOS microsensors, Proc. IEEE 86 (1998) 1660–1678.
[2] B.W. van Oudheusden, Silicon thermal flow sensors, Sens. Actuators A 30 (1992) 5–26.
[3] M. Elwenspoek, R. Wiegerink, Mechanical Microsensors, first ed., Springer-Verlag, Berlin, 2001, pp. 173–195.
[4] P. Bruschi, D. Navarrini, M. Piotto, Very low flow rate behavior of micromachined hot-plate anemometers, in: Eurosensors XVII, Guimarães, Portugal, September 21–24, 2003, pp. 272–275.
[5] F. Mayer, O. Paul, H. Baltes, Influence of design geometry and packaging on the response of thermal CMOS flow sensors, in: Eighth International Conference on Solid-State Sensors and Actuators and Eurosensors IX, Stockholm, Sweden, June 25–29, 1995, pp. 528–531.
[6] T.S.J. Lammerink, N.R. Tas, G.J.M. Krijnen, M. Elwenspoek, A new class of thermal flow sensors using $\Delta T = 0$ as a control signal, in: Proceedings of MEMS 2000, Miyazaki, Japan, January 23–27, 2000, pp. 525–530.
[7] K.A.A. Makinwa, J.H. Huijsing, A wind sensor interface using thermal sigma-delta modulation techniques, Sens. Actuators A 92 (2001) 280–285.
[8] A. Reisman, M. Berkenblit, S.A. Chan, F.B. Kaufman, D.C. Green, The controlled etching of silicon in catalyzed ethylene-diamine–pyrocatechol–water solutions, J. Electrochem. Soc. 126 (1979) 1406–1415.
[9] T. Müller, T. Feichtinger, G. Breitenbach, M. Brandl, O. Brand, H. Baltes, Industrial fabrication method for arbitrarily shaped silicon *n*-well micromechanical structures, in: The 11th International Workshop on Micro Electro Mechanical Systems, MEMS'98, Heidelberg, Germany, January 25–29, 1998, pp. 240–245.
[10] G. Yan, P.C.H. Chan, I.-M. Hsing, R.K. Sharma, J.K.O. Sin, Y. Wang, An improved TMAH Si-etching solution without attacking exposed aluminum, Sens. Actuators A 89 (2001) 135–141.
[11] S. Brida, A. Faes, V. Guarnieri, F. Giacomozzi, B. Margesin, M. Paranjape, G.U. Pignatel, M. Zen, Microstructures etched in doped TMAH solutions, Microelectron. Eng. 53 (2000) 547–551.
[12] D. Jaeggi, H. Baltes, D. Moser, Thermoelectric AC power sensor by CMOS technology, IEEE Electron Device Lett. 13 (1992) 366–368.
[13] O. Paul, O. Brand, R. Lenggenhager, H. Baltes, Vacuum gauging with complementary metal-oxide-semiconductor microsensors, J. Vac. Sci. Technol. A 13 (1995) 503–508.

Biographies

Paolo Bruschi was born in Massa, Italy, in 1964. He received the laurea degree in electronic engineering from the University of Pisa, Italy, in 1989. In 1993, he joined the Department of Information Engineering as a researcher. He is currently an associate professor of the Department of Information Engineering of the University of Pisa. His main area of interest is the development of integrated silicon sensors and actuators. He is also involved in the design of analog integrated circuits and the development of process simulators.

Alessandro Diligenti was born in 1942, La Spezia, Italy. He graduated in physics at the University of Pisa in 1969. From 1969 to 1972, he was with Centro di Studio per Metodi e Dispositivi per Radiotrasmissioni (National Research Council of Italy) at Faculty of Engineering, University of Pisa. Since 1973, he has been with the Department of Information Engineering, University of Pisa where currently he is full professor of electronic technologies. His main research interests are in the fields of solid-state devices and micromachining.

Dino Navarrini was born in Piombino, Italy, in 1975. He received the laurea degree in physics at the University of Pisa in 2000. He is currently a PhD student at the Department of Information Engineering of the University of Pisa. His research activity mainly concerns the design of integrated analog circuits and the development of integrated sensors.

Massimo Piotto was born in 1970, La Spezia, Italy. He received his laurea degree in Electronic Engineering from the University of Pisa, Italy, in 1996 and his PhD degree in electronic, computer and telecommunication engineering in 2000. From 2000 to 2001 he worked at the Department of Information Engineering of the University of Pisa as a graduated technician. Since December 2001, he has been a researcher of the section of Pisa of the "Istituto di Elettronica e di Ingegneria dell'Informazione e delle Telecomunicazioni"—National Research Council. His main research interests concern micromachining, MEMS, microelectronic and nanoelectronic devices and technologies.